EFFECT OF SPECTRAL CHANGE WIDTH IN RADIOMETRIC NORMALIZATION OF MULTITEMPORAL SATELLITE IMAGERY METHODES EFFICIENCY

Farhad Samadzadegan[1] and Seyed Hossein Seyed Pourazar[*2]
[1]Professor, Department of Geomatics Engineering, University College of Engineering, University of Tehran, Tehran, Iran; Tel: + 98-21-88986851;
E-mail: samadz@ut.ac.ir

[2]Graduate student, Department of Geomatics Engineering, University College of Engineering, University of Tehran, Tehran, Iran; Tel: + 98-21-88986851;
E-mail: h.pourazar@ut.ac.ir

KEY WORDS: Relative Radiometric Normalization, Linear Radiometric Normalization, RMSE, UQI.

ABSTRACT: Multitemporal satellite optical images of the same terrain are very applicable in monitoring and quantifying large scale land cover change over time. These images are confounded in terms of radiometric consistency due to differences in sensor calibration parameters, illumination, geometric condition and variation in atmospheric effects. To analyze these images, it is necessary to omit mentioned differences. Relative radiometric normalization is used to prepare these images for stated applications. In this paper, different relative radiometric normalization methods are compared with each other. Images of Landsat-5 thematic mapper (TM) and Landsat-7 enhanced thematic mapper plus (ETM+) captured from Iran are used for this comparison. The results of various techniques have been evaluated with both visual inspection and statistical analysis i.e. Root Mean Square Error (RMSE) and Universal Quality Indicator (UQI) value between each pair of analogous band. Obtained results show intensity value of spectral changes affects quality of normalization. In images which have small area with intensified spectral changes, MS, HM and MM methods produce better results; while in images with intensified changes covering large area, PIF method generates the best results. Also among mentioned methods, MS method is the most stable with respect to changes.

1. INTRODUCTION

The Reflected irradiance of the features is influenced by many factors while acquiring remote sensing images, such as sensor itself, solar elevation angle, topography, atmospheric and so on, and lead to the same features with different spectral information in Multitemporal images (Xiaoke et al. 2009). This causes many challenges in Multitemporal images analysis such as change detection and Simultaneous analyses of images in order to model variety Phenomena. Radiometric correction has become an indispensable and important part in image processing and plays a key role in remote sensing data analysis (Xiaoke et al. 2009; Janzen et al. 2006).
Radiometric correction of satellite imagery falls into two broad categories, namely absolute and relative (Xiaoke et al. 2009; Janzen et al. 2006; Chen et al. 2005). Absolute radiometric correction is aimed towards extracting the absolute reflectance of scene targets at the surface of the earth (Chen et al. 2005). The application of these models to a satellite scene often requires atmospheric and sensor properties for the acquisition date of that scene (Pudale & U. V. Bhosle 2007). Relative radiometric correction uses gray value of features in Multitemporal images instead of radiance or reflectance. Relative radiometric correction matches the calibration between other images and the main image after the main image is selected (Xiaoke et al. 2009). The relative radiometric correction method can correct noise deriving from the atmosphere, sensor, and other sources in one process, and is therefore widely used. The relative approach to radiometric correction, known as relative radiometric normalization, is preferred because no in situ atmospheric data at the time of satellite overpasses are required (Yang & Lo 2000)
Recently, extensive researches about relative normalization of satellite imagery and its impact in various applications has been done (Janzen et al. 2006; Pudale & U. V. Bhosle 2007; Ya'allah & Saradjian 2005; Biday & U. Bhosle 2010; Yuan & Elvidge 1996; Canty & Nielsen 2008). Yuan and Elvidge (1996) investigated seven linear relative normalization methods. They got the best results from methods using unchanged targets to compute coefficients. Pudale and Bhosle (2007) used seven methods investigated by Yuan and Elvidge (1996) to normalize a pair of images of Resourcesat1 LISS III sensor. Results showed Simple Regression (SR), No-Change (NC) and Dark-Brightness (DB) methods not only had good performance but also were the same. Du et al (2002) got regression coefficients applying principle component analysis. As can be seen, efficiency of relative radiometric normalization methods hasn't been explored in mentioned investigations, where radiometric changes are high. In this study we want to get effect of high radiometric changes in normalization process. So in this study Haze Correction (HC), Minimum-Maximum (MM), Simple Regression (SR), Mean Standard Deviation (MS), No-Change regression (NC), Pseudo Invariant Feature (PIF) and histogram Matching (HM) methods are implemented and investigated.

2. RELATIVE RADIOMETRIC NORMALIZATION

Image normalization described in literature can be categorized into three overall categories: statistical methods (i.e., standard deviation method); the histogram matching method (HM); linear radiometric normalization methods (i.e., PIF, DB and NC) (Biday & U. Bhosle 2010). Histogram matching method and six linear radiometric normalization methods are described in this section.

2.1 Linear Radiometric Normalization

Linear Radiometric Normalization methods assume that radiometric relationships between the target image and the base image are linear. The objective of linear spectral normalization is to rectify subject image X to reference image Y through a linear transformation (Pudale & U. V. Bhosle 2007):

$$y'_k = a_k x_k + b_k \tag{1}$$

where x_k is the DN of band k in image X on date1, y'_k is the normalized DN of band k on date1, and a_k, b_k, are normalization constants for band k.
Relative radiometric normalization (RRN) process can broadly divided into two steps, first is selection of normalization targets and then determining normalization coefficients (Pudale & U. V. Bhosle 2007). One of them is, the patterns on the normalization targets should not change over time when viewed on the image display screen; and a set of targets must have a wide range of grey values (Pudale & U. V. Bhosle 2007; Biday & U. Bhosle 2010).
In order to determine optimum method in this study six aforementioned methods are evaluated. Four first methods consider cover of radiometric range also they use all pixels which have the same position to compute regression coefficient while two other methods i.e. NC and PIF use selected pixels.

2.1.1 Haze correction (HC): Haze correction assumes that pixels having zero reflectance (darkest 0.1% of the image pixels) should have the same minimum DN values on both subject and reference images. The HC normalization coefficients are:

$$a_k = 1 \quad , \quad b_k = y_{k_{min}} - x_{k_{min}} \tag{2}$$

where $x_{k_{min}}$ and $y_{k_{min}}$ are the haze values in band k in images X and Y, respectively.

2.1.2 Minimum-maximum (MM): This method normalizes the subject image so that it will have the same minimum and maximum DN values as those of the reference image in all bands. The normalization coefficients for the minimum-maximum method are (Yuan & Elvidge 1996):

$$a_k = \frac{y_{k_{max}} - y_{k_{min}}}{x_{k_{max}} - x_{k_{min}}} \quad , \quad b_k = y_{k_{min}} - a_k x_{k_{min}} \tag{3}$$

where $x_{k_{min}}$, $x_{k_{max}}$, $y_{k_{min}}$ and $y_{k_{max}}$ are the minimum and maximum DN values of band k for two dates. The MM values for the two dates of imagery were selected as the DN thresholds required to isolate the upper and lower 0.1% of the image data.

2.1.3 Mean-standard deviation (MS): This method normalizes image X such that subject image X and reference image Y have the same mean and standard deviation in all bands. Suppose $\bar{x}_k$ and $\bar{y}_k$ are the means, S_{x_k} and S_{y_k} are the standard deviations of x_k and y_k, respectively. Then the MS normalization coefficients are then derived as (Yuan & Elvidge 1996):

$$a_k = \frac{S_{y_k}}{S_{x_k}} \quad , \quad b_k = \bar{y}_k - a_k \bar{x}_k \tag{4}$$

2.1.4 Simple Regression (SR): In this method, the subject image is regressed against the reference image in each band. Simple regression normalization uses least-squares to derive the normalization coefficients. The SR normalization coefficients are solved from the least-squares regression equation (Biday & U. Bhosle 2010; Yuan & Elvidge 1996):

$$Q = \sum_{\text{scene}} (y_k - a_k x_k - b_k)^2 = \min. \tag{5}$$

$$a_k = \frac{S_{x_k y_k}}{S_{x_k x_k}} \quad , \quad b_k = \bar{y}_k - a_k \bar{x}_k \tag{6}$$

2.1.5 Pseudo invariant Features (PIF): This method is developed using spectrally pseudo invariant features, such as impervious roads, rooftops and parking lots, to allow inter comparisons between a slave image and a master image by calculating an image based linear regression. The pseudo-invariant features are extracted by analyzing the infrared to red ratio of the master and slave images to identify pixels having low green vegetation cover and a NIR threshold to eliminate water pixels (Chen et al. 2005; Biday & U. Bhosle 2010; Yuan & Elvidge 1996).

$$\text{PI set} = \{ (\text{Band5}/\text{Band3}) < T1 \ \& \ \text{Band5} > T2 \} \tag{7}$$

Let the means and standard deviations of the selected pseudo-invariant sets for the two dates to be $\bar{y}^{(pi)}$, $\bar{x}^{(pi)}{}_k$, $S^{(pi)}{}_{y_k}$, $S^{(pi)}{}_{x_k}$. The PIF normalization coefficients are:

$$a_k = \frac{S^{(pi)}{}_{y_k}}{S^{(pi)}{}_{x_k}} \ , \ b_k = \bar{y}^{(pi)}{}_k - a_k \bar{x}^{(pi)}{}_k \tag{8}$$

2.1.6 No-change regression (NC): A no-change set is determined based on correlation in frequency domain (Biday & U. Bhosle 2010). Its stages are as follows:

- The master and slave images are divided into rectangular blocks of size 16×16 pixels;
- Normalized correlation between two corresponding blocks is calculated;
- A block is assumed to belong to the no-change set if it has normalized correlation in all bands greater than 0.9.

Thus if the no-change subset NC is identified, one can solve the least-squares equation to obtain the normalization coefficients:

$$a_k = \frac{S^{(nc)}_{x_k y_k}}{S^{(nc)}_{x_k x_k}} \quad , \quad b_k = \bar{y}^{(nc)}_k - a_k \bar{x}^{(nc)}_k \tag{9}$$

where $S^{(nc)}_{x_k x_k}$, $S^{(nc)}_{x_k y_k}$ are the sample variance and covariance for the subset NC on two dates.

2.2 Histogram Matching (HM)

Histogram matching is a method for converting one image into another image with a considered histogram. In normalization with this method, interested histogram is the histogram of master image. The goal of this method is converting of slave image into an image which its histogram is similar to that of the master image. Its stages are as follows (Richards & Jia 2006):

- Computation of master and slave histogram;
- Computation of cumulative histogram from computed histograms;
- Generation of Look Up Table (LUT);
- Interpolation of new value for each pixel of LUT.

$$y = g^{-1}(z) \ , \quad z = f(x) \text{ or } y = g^{-1}\{f(x)\} \tag{10}$$

3. ASSESSMENT CRITERIA

In this study, image quality is used to assessment of normalized image. Image quality can be determined in two ways i.e. Qualitative and quantitative methods. Qualitative methods are based on the assessment of images by the human observer (Thomas & Wald 2006; D. Zhang 2006; Y. Zhang 2008; Shi et al. 2005). In this method, observer can obtain image quality by visual comparison of colors among corrected, master and slave images (Y. Zhang 2008; Alparone et al. 2007).

Due to the limitations of qualitative assessment methods, quantitative evaluation methods have been used more. These methods have predetermined quality indicators. Among different quantitative methods, in this paper, the results

are assessed by Root Mean Square Error (RMSE) and Universal Quality Index (UQI).
RMSE is one of the most applicable quantitative criteria to compute spectral differences between two images. This criterion is calculated using equation (11).

$$RMSE = \sqrt{\frac{\sum_{k=1}^{n} (\hat{y}_k - y_k)^2}{n}} \tag{11}$$

where y_k and $\hat{y}_k$ are the digital number (DN) of band k in master and normalized images, respectively. In this research, disadvantage of this metric has been shown by the results. Therefore, other quantitative metric was used.
UQI has three components which model loss of correlation, Illumination distortion and contrast distortion. If parameters x_i and y_i are considered as a master image and processed image, respectively, UQI can be calculated as follows:

$$Q = \frac{\sigma_{xy}}{\sigma_x.\sigma_y} \cdot \frac{2.\overline{x}\overline{y}}{\overline{x}^2 + \overline{y}^2} \cdot \frac{2\sigma_x.\sigma_y}{\sigma_x^2 + \sigma_y^2} \tag{12}$$

where $\overline{x}$ and $\overline{y}$ are mean, while σ_x and σ_y are variance of two images. Q index is bounded in [-1,1] and its maximum value (Q=1) is achieved when x and y became equal (x=y).

4. EXPERIMENT AND RESULTS

In order to evaluate seven relative normalization methods introduced in part 2, two sets of Landsat images were used. The first image set contains the first, second, third and fifth bands of Landsat TM and ETM+ images, taken in 2000 (Figure 1-A) and 2006 (Figure 1-B), which covers the east area of Tehran, Iran. There aren't any clouds in these images and also land cover changes are small. A small part of images is considered to contain high spectral changes due to draining the water of the lake. The next image set is the first band until third one and the fifth band of Landsat ETM+ images of the southern part of the Urmia lake that have been captured in 1989, (Figure 2-A) and 2000 (Figure 2-B), respectively. In this set, severe spectral changes which have been caused by drying of the lake water, has a large area.

4.1 Evaluation of Results

In the HC, MM, SR and MS methods, as stated in the previous sections, all pixels are used to determine the coefficients. In the PIF method, the T1=3 and T2=100 thresholds were used. About NC method, In order to select ١٥×١٥ blocks, correlation 0.90 was used as threshold. Obtained Coefficients from each of the six methods of linear relative normalization are given in Table 1:

Table 1. Normalization coefficients obtained for sets of images by the 6 relative linear normalization methods.

	First image set						second image set					
Band	**1**		**2**		**3**		**1**		**2**		**3**	
Coefficients	**a**	**b**	**a**	**b**	**a**	**b**	**a**	**b**	**a**	**b**	**a**	**b**
HC	1	19	1	15	1	13	1	-38	1	10	1	8
MM	0.626	3.07	0.595	8.48	0.608	8.06	0.851	-26.05	1.125	6.88	0.957	8.78
SR	1.444	3.19	1.446	4.13	1.418	10.34	0.140	56.76	0.304	58.00	0.308	68.34
MS	0.608	7.16	0.611	6.09	0.621	4.48	0.505	4.69	0.989	12.37	0.824	18.59
NC	1.463	-0.78	1.417	2.08	1.447	1.5	0.518	3.74	1.162	3.03	0.97	8.77
PIF	1.605	-9.7	1.649	-12.6	1.654	-13.77	0.332	28.20	0.666	34.28	0.583	44.39

Normalized images by each of the seven aforementioned methods are displayed in Figure 1 and 2. It is clear that in images with the spectral changes in large area, all methods except the HC were good. In other word, identification of the best method isn't possible, since the results are quite similar. But when the rate of these changes is high, the difference in performance of methods is visually quite visible. The RMSE and UQI of these images are given in Table 2; also the graphs of these values with their average are presented in Figure 3.

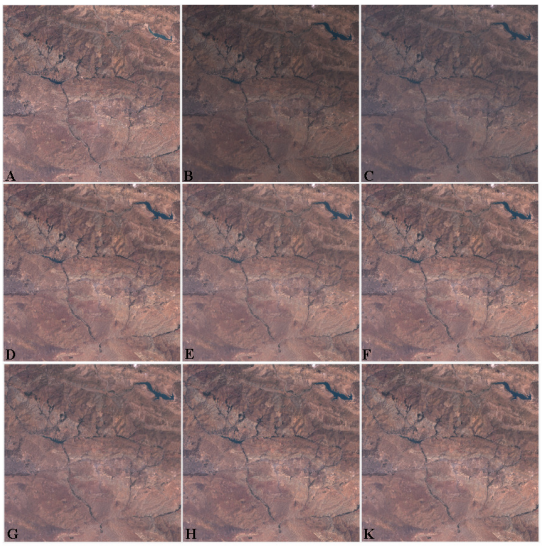

Figure 1. A) Landsat ETM+ image obtained from Tehran in 2000; B) Landsat ETM+ image obtained from Tehran in 2006; C) B image normalized by HC method; D) MM method; E) SR method; F) MS method; G) NC method; H) PIF method; and K) HM method.

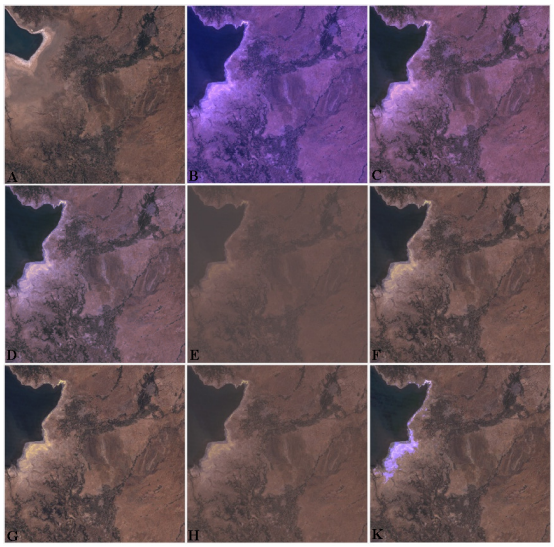

Figure 2. A) Landsat TM image obtained from Urmia Lake in 1989; B) Landsat ETM+ image obtained from Urmia Lake in 2000; C) HC method; D) B image normalized y MM method; E) SR method; F) MS method; G) NC method; H) B image PIF method; and K) HM method.

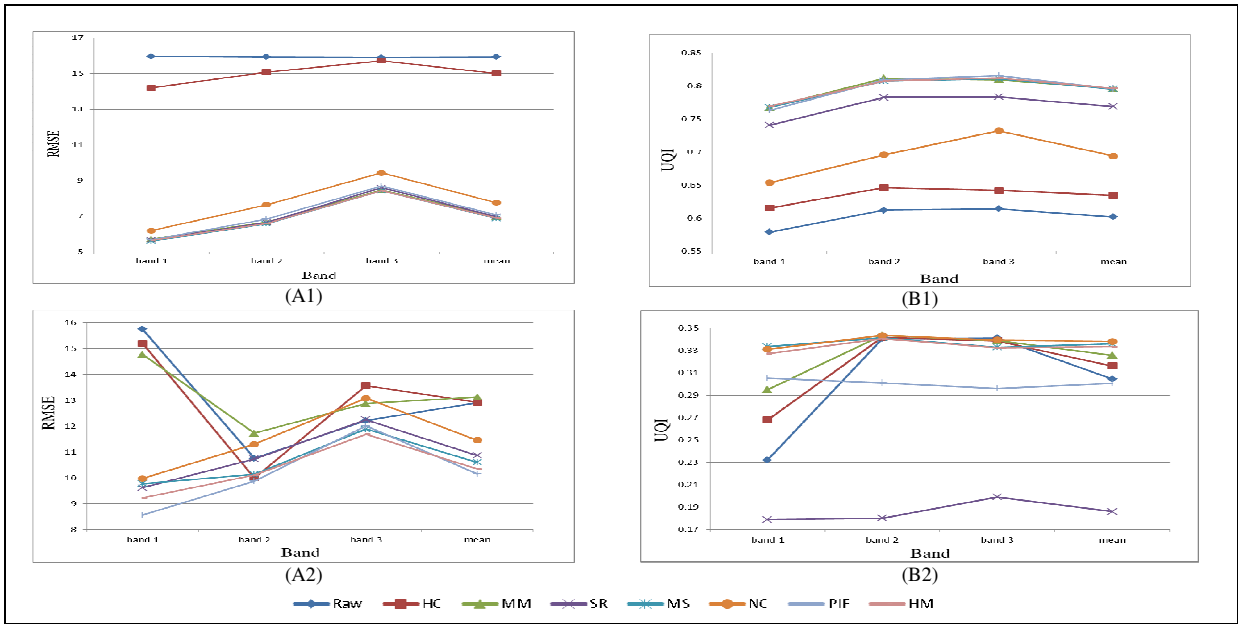

Figure 3. Graphs of: A1) RMSE for normalized image in first image set; B1) UQI for normalized image in first image set; A2) RMSE for normalized image in second image set; B2) RMSE for normalized image in second image set.

Table 2.Values of RMSE and UQI in two images set for row and normalized images.

	First image set						**second image set**					
	RMSE			UQI			RMSE			UQI		
Band	**1**	**2**	**3**	**1**	**2**	**3**	**1**	**2**	**3**	**1**	**2**	**3**
Row	15.901	15.9268	15.951	0.5786	0.6117	0.6139	15.751	10.756	12.214	0.2320	0.3405	0.3411
HC	15.716	15.072	14.1956	0.6152	0.6460	0.6419	15.196	9.9887	13.572	0.2679	0.3419	0.3387
MM	8.4757	6.6720	5.7223	0.7672	0.8116	0.8091	14.772	11.728	12.874	0.2951	0.3436	0.3389
SR	8.5997	6.6568	5.6727	0.7404	0.7823	0.7832	9.6241	10.733	12.247	0.1788	0.1801	0.1990
MS	8.4272	6.5848	5.6093	0.7672	0.8075	0.8109	9.7788	10.142	11.885	0.3335	0.3415	0.3329
NC	9.4380	7.6456	6.1948	0.6533	0.6957	0.7322	9.9807	11.300	13.082	0.3337	0.3447	0.3389
PIF	8.6973	6.8473	5.6887	0.7627	0.8089	0.8155	8.5625	9.8852	12.012	0.3053	0.3012	0.2961
HM	8.4416	6.5983	5.6413	0.7693	0.8073	0.8117	9.2321	10.756	11.680	0.2320	0.3406	0.3411

According to the diagrams depicting in Figure 3-A1 and the values presented in Table 2, it is clear that RMSE and UQI are improved in the first image set by all methods. It is also observed that the HC has the highest RMSE in all bands of these images, and the lowest UQI, therefore it had the weakest results. With regard to the others, Performance of them was good and similar. According to these criteria, performance of them from good to bad performance is: HC<NC<SR<PIF<MM<HM<MS. Weak performance of NC is associated with bad selection of pixels from spectral distribution. In fact, the NC and the PIF strongly depend on the selected targets.
The observed results in the second set of images indicate a poor performance of HC. According to visual inspection and UQI metric, MM performance is better than HC, but its RMSE is high. The graph of Figure 3-B2 shows that PIF has had lowest RMSE and highest UQI. According to Table 2, it is obvious that RMSE without other criterion is not suitable for assessment of the normalization methods. For example, obtained image by the SR method has produced the worst visual quality, while it has had good RMSE and worst UQI.

5. CONCLUSION

In this paper, seven methods of image normalization were implemented and evaluated on two sets of Multitemporal images. The main purpose of this study was to investigate performance of these methods in the circumstances having wide spectral changes. Therefore, we used two sets of images with little and large spectral changes. Among the methods used, the HC results were the weakest. MS method provided a good result in both sets of images. In the other word, this method was stable in various ground conditions. Efficiency of NC and PIF methods strongly depends on considered area, because the results of them are significantly affected by selecting of targets. When spectral change values were low, HM method had a good result, but in area where spectral changes are large and intensified, such as second image set, change values were unrealistic, specifically for pixels having minimum and maximum gray value. Last note of this study is about used quantitative criteria. Although RMSE is used in many studies as a quantitative criterion, this paper showed that it isn't efficient to use it alone. So, for improving of quantitative investigation UQI is proposed. According to obtained results, a method has a good efficiency if it has the best values of both RMSE and UQI. So in the feature study, the goal is to find a criterion for evaluating normalized images which can correctly evaluate relative normalization.

REFERENCES

Alparone, L. et al., 2007. Comparison of pansharpening algorithms: Outcome of the 2006 GRS-S data-fusion contest. Geoscience and Remote Sensing, IEEE Transactions on, 45(10), pp.3012–3021.
Biday, S.G. & Bhosle, U., 2010. Radiometric Correction of Multitemporal Satellite Imagery. Journal of Computer Science, 6(9), pp.940–949.
Canty, M.J. & Nielsen, A.A., 2008. Automatic radiometric normalization of multitemporal satellite imagery with the iteratively re-weighted MAD transformation. Remote Sensing of Environment, 112(3), pp.1025–1036.
Chen, X., Vierling, L. & Deering, D., 2005. A simple and effective radiometric correction method to improve landscape change detection across sensors and across time. Remote sensing of environment, 98(1), pp.63–79.
Du, Y., Teillet, P.M. & Cihlar, J., 2002. Radiometric normalization of multitemporal high-resolution satellite images with quality control for land cover change detection. Remote Sensing of Environment, 82(1), pp.123–134.
Janzen, D.T., Fredeen, A.L. & Wheate, R.D., 2006. Radiometric correction techniques and accuracy assessment for Landsat TM data in remote forested regions. Canadian Journal of Remote Sensing, 32(5), pp.330–340.
Pudale, S.R. & Bhosle, U.V., 2007. Comparative study of relative radiometric normalization techniques for Resourcesat1 LISS III Sensor Images. In iccima. pp. 233–239.
Richards, J.A. & Jia, X., 2006. Remote sensing digital image analysis: an introduction, Springer Verlag.
Shi, W. et al., 2005. Wavelet-based image fusion and quality assessment. International Journal of Applied Earth Observation and Geoinformation, 6(3-4), pp.241–251.
Thomas, C. & Wald, L., 2006. Comparing distances for quality assessment of fused products. In Proc. 26th EARSeL Annu. Symp. New Develop. Challenges Remote Sens. pp. 101–111.
Xiaoke, Z. et al., 2009. Radiometric correction based on Multitemporal SPOT satellite images. In Wireless Communications & Signal Processing, 2009. WCSP 2009. International Conference on. pp. 1–6.
Yang, X. & Lo, C.P., 2000. Relative radiometric normalization performance for change detection from multi-date satellite images. Photogrammetric Engineering and Remote Sensing, 66(8), pp.967–980.
Ya'allah, S.M. & Saradjian, M.R., 2005. Automatic normalization of satellite images using unchanged pixels within urban areas. Information Fusion, 6(3), pp.235–241.
Yuan, D. & Elvidge, C.D., 1996. Comparison of relative radiometric normalization techniques. ISPRS Journal of Photogrammetry and Remote Sensing, 51(3), pp.117–126.
Zhang, D., 2006. Information theoretic criteria for image quality assessment based on natural scene statistics. MSc Thesis. University of Waterloo.
Zhang, Y., 2008. Methods for image fusion quality assessment–A review, comparison and analysis. The International Archives of the Photogrammetry, Remote Sensing and Spatial Information Sciences, 37, pp.1101–1109.